# Identity, Energy, and Environment of Interfacial Water Molecules in a Micellar Solution

**Subrata Pal,[†] Sundaram Balasubramanian,*[,‡] and Biman Bagchi*[,†]**

*Chemistry and Physics of Materials Unit, Jawaharlal Nehru Centre for Advanced Scientific Research, Jakkur, Bangalore 560064, India, and Solid State and Structural Chemistry Unit, Indian Institute of Science, Bangalore 560012, India*

*Received: October 31, 2002; In Final Form: April 2, 2003*

The structure and energetics of interfacial water molecules in the aqueous micelle of cesium perfluorooctanoate have been investigated, using large-scale atomistic molecular dynamics simulations, with the primary objective of classifying them. The simulations show that the water molecules at the interface fall into two broad classes: bound and free, present in a ratio of 9:1. The bound water molecules can be further categorized on the basis of the number of hydrogen bonds (one or two) that they form with the surfactant headgroups. The hydrogen bonds of the doubly hydrogen-bonded species are found to be, on the average, slightly weaker than those in the singly bonded species. The environment around interfacial water molecules is more ordered than that in the bulk. The surface water molecules have substantially lower potential energy, because of interaction with the micelle. In particular, both forms of bound water have energies that are lower by ∼2.5−4.0 kcal/mol. Entropy is found to play an important role in determining the relative concentration of the species.

## 1. Introduction

The structure and dynamics of fluids near interfaces can be vastly different from their bulk behavior.[1−3] Organic liquids often tend to be structured near solid surfaces, with typically higher local density than that in the bulk. The presence of such a solid surface induces layering of the molecules of the fluid, which manifests itself as oscillations in the density. Unlike liquids near a solid surface, liquids at soft interfaces could exhibit different behavior.[4] Such soft interfaces include macromolecules of biological interest, such as proteins, DNA, and organized assemblies such as micelles, reverse micelles, phospholipid bilayers, and a host of other systems, where the natural solvent is water.[5−8] Water molecules at the interface of such systems exhibit slow dynamics, whose origin is now a subject of intense discussion.[9−12] Recent time-domain spectroscopic measurements have shown that the dynamics of interfacial water can be considerably slower than their counterparts in bulk water, sometimes slower by even more than 2 orders of magnitude.[13,14] For example, although the reorientation of water molecules and solvation of ions or dipoles in bulk water proceeds with an average time constant of less than a picosecond, the same at macromolecular surfaces gets extended to hundreds of picoseconds.[7,13−15] This slow dynamics can play an important role in many natural and biological processes, such as electron-transfer reactions, the gating of ions across membranes, and molecular recognition in hydrophobic pockets of proteins and protein aggregation.[8]

Experiments and simulations performed over the past decade have contributed to our understanding in this area, and a general picture of the processes involved is beginning to emerge now. Nandi and Bagchi proposed a phenomenological model to explain the observed slow dielectric relaxation of aqueous protein solutions.[16] The model envisages the existence of interfacial water molecules in two different states: one *bound* and the other *free*. The former was assumed to form hydrogen bonds with the hydrophilic groups on the macromolecule, whereas the latter retain their bulk characteristics. They interpreted the dielectric relaxation spectra in terms of a dynamical equilibrium between these two states of water. The slow time constant that emerges is essentially the time constant of transition from the bound water to the free state of water. Thus, the Nandi−Bagchi (NB) theory is critically dependent on the assumption of the presence of bound and free water molecules in the layer.

Recently, we have performed extensive computer simulations of the aqueous micelle of cesium perfluorooctanoate (CsPFO). These simulations have confirmed the slow reorientation of interfacial water molecules,[17,18] and the slow solvation of cesium ions near the micellar interface.[19,20] In a preliminary study, we have attributed the origin of the slow dynamics to the long-lived hydrogen bonds that an interfacial water molecule makes with the polar headgroup (PHG).[21]

The purpose of this study is different. Here, we concentrate on the identity, binding, and energetics of the water molecules in the hydration layer and also provide details of the structure and thermodynamics of the interfacial species that determine their dynamics. The calculations have been performed for a micelle composed of CsPFO surfactant molecules in water at a temperature of 300 K. Most of the earlier work on micellar solutions has focused on the structure of the solvent, from the perspective of the hydrophilic headgroups.[22−24] In regard to the previously discussed experiments, one needs to reformulate the data in terms of the structure around the interfacial water. This aspect constitutes the present work. The simulations clearly reveal the existence of *three* different types of interfacial water molecules. One of them is not hydrogen-bonded at all to any PHG and is bonded only to other water molecules, whereas the other two species are hydrogen-bonded to either one or two PHGs. This distinction in structure is also reflected in their energetics. Most notably, the bound water molecules have

* Authors to whom correspondence should be addressed. E-mail: bala@jncasr.ac.in (S.B.), bbagchi@sscu.iisc.ernet.in (B.B.).
† Indian Institute of Science.
‡ Jawaharlal Nehru Centre for Advanced Scientific Research.

10.1021/jp022349+ CCC: $25.00 
Published on Web 05/10/2003

considerably lower energy at the interface, and entropic considerations must be included to account for the relative concentrations of the three species.

The remainder of the paper is divided as follows. In the following section, we briefly sketch the details of the simulation. Results on the local environment around interfacial water are presented subsequently, along with data on the state and pair energies of the three species of interfacial water. Conclusions derived from our work are presented later.

## 2. Details of Simulation

As already mentioned, the surfactant is pentadecafluorooctanoate, with cesium being the counterion. The CsPFO−$H_2O$ system has been well studied experimentally[25,26] and is regarded as a typical binary to exhibit micellization.[27] The amphiphiles are believed to form disk-shaped (oblate ellipsoid) micelles, stable over an extensive range of concentration and temperature. The critical micelle concentration is ∼0.02 (weight fraction) of CsPFO in water. The molecular dynamics simulations were performed in the NVT ensemble for an aggregate of 62 CsPFO molecules in 10 562 $H_2O$ molecules at 300 K. The initial configuration of the micelle was built to mimic experimental data pertaining to its size and shape.[26] The potential for water molecules is the extended simple point charge (SPC/E) model;[28] the counterions carry a unit positive charge, which is compensated by a +0.4 *e* charge on the carbon atom of the octanoate headgroup and a −0.7 *e* charge on each of the oxygen atoms of the headgroup.[22] The surfactant is modeled with explicit fluorine atoms and interactions between the fluorocarbon tails were obtained from the work of Sprik et al. on poly(tetrafluoroethylene).[29] Other details of the potential parameters are provided elsewhere.[17] The equations of motion were integrated with the reversible reference system propagator algorithm (RESPA) scheme,[30] using the PINY-MD package[31] with an outer time step of 4 fs. Coulombic interactions were treated using the particle mesh Ewald method. The linear dimensions of the simulation cell at 300 K were 80.6, 80.6, and 52.1 Å. Details of the simulations can also be found elsewhere.[17−21] The analyses reported here were conducted from different sections of a 3-ns trajectory. They include calculations of various pair-correlation functions, angle distribution functions, monomer and pair energy distribution functions. Spherically averaged pair-correlation functions are not quite effective in determining the structure in inhomogeneous and anisotropic systems such as ours. Yet, peak positions and minima in them can provide information on the local geometry around interfacial water molecules.

The results pertaining to interfacial water are presented in comparison to a system of bulk water. The simulation of bulk water contained 256 molecules of the SPC/E type at a temperature of 300 K and a density of 1.02 g/cm$^3$.

Acronyms used in this work are described as follows: (i) PHG, polar headgroup that denotes the carboxylate group of the surfactant; (ii) PHGO, oxygen atom of the polar headgroup; (iii) WO, oxygen atom of the water molecule; (iv) IWO, oxygen atom of the interfacial water molecule; (v) WH, hydrogen atom of the water molecule; (vi) W−PHG, hydrogen bond between a water molecule and a polar headgroup of surfactant; (vii) IFW, interfacial free water molecule that does not form a hydrogen bond with any PHG; (viii) IBW1, interfacial bound water molecule that forms one hydrogen bond to a PHG; (ix) IBW2, interfacial bound water molecule that forms two hydrogen bonds to two different PHGs.

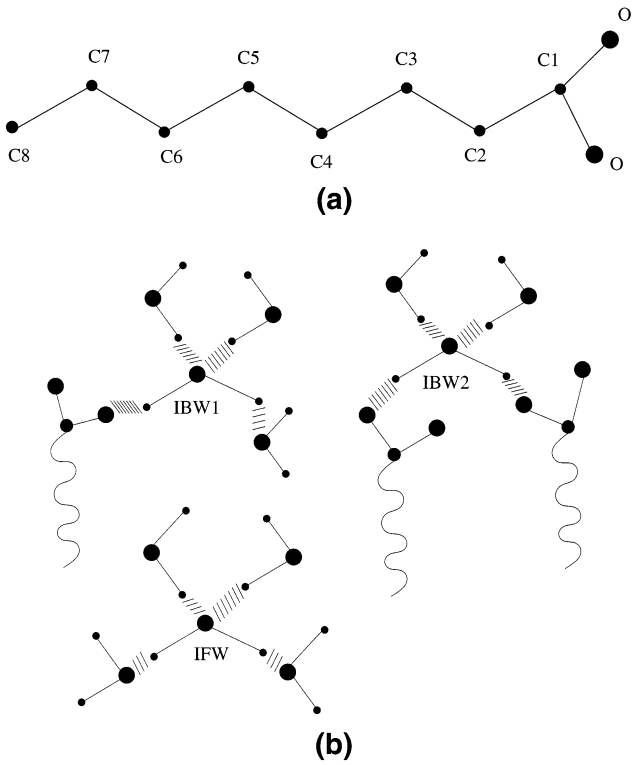


**Figure 1.** 1. (a) Schematic representation of the surfactant molecule with atom labels; F atoms are not shown. (b) Schematic representation of the bonding pattern of the three types of interfacial water molecules (namely, IFW, IBW1, and IBW2). IBW1 and IBW2 types of water molecules form hydrogen bond(s) with the polar headgroup of the surfactant molecule(s). IFW molecules, although present in the interfacial region, do not form any hydrogen bond with the surfactant and, instead, are bonded purely to other water molecules in the vicinity.

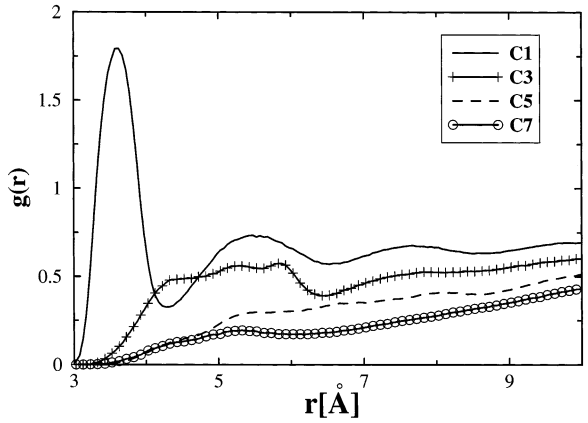


**Figure 2.** Pair correlation functions of various carbon atoms along the backbone of the surfactant to the oxygen atom of water molecules in the micellar solution. Alternate points are dropped in curves with symbols for clarity.

## 3. Results and Discussion

**3.1. Characterization of the Interface.** To understand the structure around interfacial water molecules, we need first to locate them, with respect to the atoms constituting the micelle. A schematic of the labeling of the backbone atoms in a surfactant molecule is shown in Figure 1a, whereas Figure 1b shows a schematic representation of the bonding pattern of the three types of interfacial water molecules.

In Figure 2, we show the spherically averaged pair-correlation function ($g(r)$) of water molecules around a given central carbon atom. The figure contains data for alternate carbon atoms along

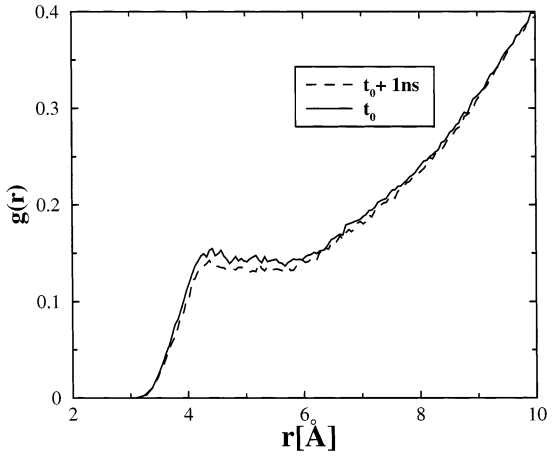


**Figure 3.** Radial distribution function of the last carbon atom (C8) in the surfactant tail and the oxygen atom of water molecules at two instances separated in time by 1 ns.

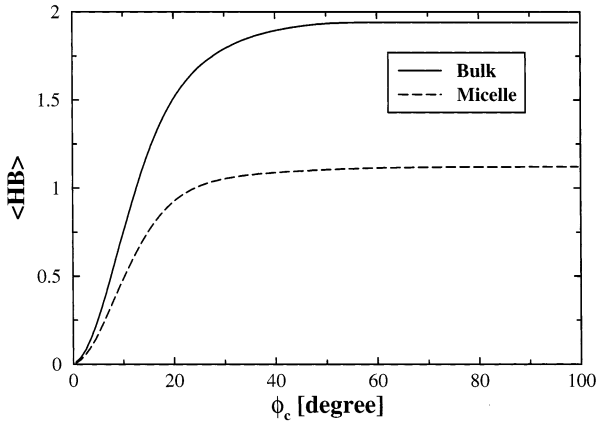


**Figure 4.** (—) Average number of water−water hydrogen bonds per water molecule in bulk water and (− − −) average number of W−PHG hydrogen bonds per bound water molecule in the micellar solution, plotted as a function of the critical OOH angle, $\phi_c$, employed in the definition of the hydrogen bond.

the backbone of the surfactant. Water molecules are seen to be structured well around the headgroup carbon atom (with the label C1), whereas the structure is lost rapidly as one moves down the tail of the amphiphile. Water molecules are thus seen to penetrate into the micelle up to two or three $CF_2$ groups, which is consistent with earlier simulations of micellar solutions.[22,23] The structured water in the first coordination shell of the C1 atom is termed "interfacial water" in this paper. The stability of the micelle critically depends on the extent of penetration of water. We demonstrate the stability of the simulated micelle by comparing the C8−water $g(r)$ calculated at two different times during the simulation, which are separated by a time interval of 1 ns. This is shown in Figure 3, and the almost-identical behavior of the pair-correlation functions shows that the penetration of water into the micelle has reached a stationary state, at least on these time scales. It is seen that the nearest water molecule to the C8 atom is a distance of 4 Å away. This proximity might seem somewhat alarming initially but can be easily rationalized on the basis of the fluctuations in the arrangement of neighboring surfactant molecules, with respect to each other; i.e., given the roughness of the micellar surface, water molecules can, at rare occasions, be found close to the tail region of surfactant molecules. The end-to-end length of the surfactant, which is defined as the distance between the C1 and C8 atoms, is also not large. The preferred conformation of such a perfluorinated chain is helical.[29] The distribution of this end-to-end length in the simulated micelle (not shown here) peaks at 7.0 Å, which indicates that the water molecules have penetrated, at most, only 3 Å into the micelle. In addition, the amplitude of such occurrences is very low.

**3.2. Definition of the Water−PHG Hydrogen Bond.** We define an interfacial water as one that is within the first coordination shell of the C1 atom of the PHG, i.e., within a distance of 4.35 Å. In our system (which contains 62 surfactant molecules and 10 562 water molecules), on the average, 363 water molecules constitute this hydration layer. We then explored the possibility of whether this hydration layer indeed contains two types of waters: those which are hydrogen-bonded to a PHG through the PHGO atom, and others that are not. The former can be termed as "bound", denoted by IBW, whereas the latter can be called "free", denoted by IFW.[16] The bound water molecules can be further distinguished on the basis of the number of hydrogen bonds that they make with the PHGs of the surfactant. This can either be one or two, and, thus, all interfacial water molecules can be classified into three types: in this article, we denote them as IFW, IBW1, and IBW2, depending on whether the interfacial water molecule has zero, one, or two hydrogen bonds, respectively, with the headgroup oxygen atoms.

It is difficult to define objectively the presence of an intermolecular bond in classical simulations of liquids with empirical potentials. The definition of a hydrogen bond between water molecules in liquid water, or that between an interfacial water molecule and the PHG, fall under this category.[32−38] In the choice of a distance criterion to define the hydrogen bond, one can be guided by the pair-correlation function, and a suitable choice would be the first minimum of the function. However, the hydrogen bond is reasonably directional,[39] and, hence, one may have to include an orientational criterion in the bond definition as well. This is traditionally included as a condition on the OOH angle. Thus, a pair of water molecules are said to be hydrogen-bonded if their oxygen atoms are within 3.5 Å, and if the angle at any of the oxygen atoms that are involved in the bonding is within 30°. In pure water, the choice of the critical angle has been made by studying the average number of hydrogen bonds per water molecule as a function of the critical OOH angle.[35] The corresponding function in the micellar solution is the average number of W−PHG hydrogen bonds per bound water molecule, plotted as a function of the critical PHGO−WO−WH angle; this is displayed in Figure 4. The figure also includes the relevant function in pure water for comparison. The two functions exhibit almost-identical behavior, with the only difference being that the average number of hydrogen bonds of the W−PHG type at the largest critical angle is 1.12, whereas that of the water−water type in pure water is 1.94 per water molecule. The former value is consistent with the expected number of W−PHG bonds calculated on the basis of the concentration of IBW1 and IBW2 species (see later discussion). The W−PHG function saturates at an angle of 55°. In a recent interesting study, Berkowitz and co-workers introduced a condition on the OHO angle in the definition of the hydrogen bond between a water molecule and a surfactant in a micellar solution.[40] A lower limit of 140° for the OHO angle, and a cutoff distance between the bonded oxygen atoms were both considered to determine the bondedness to the surfactant. A particular choice of the angle, although convenient, does not, however, appear to have any additional advantage, compared to other choices, on the basis of energetic considerations. In addition, although the condition of an O−O distance

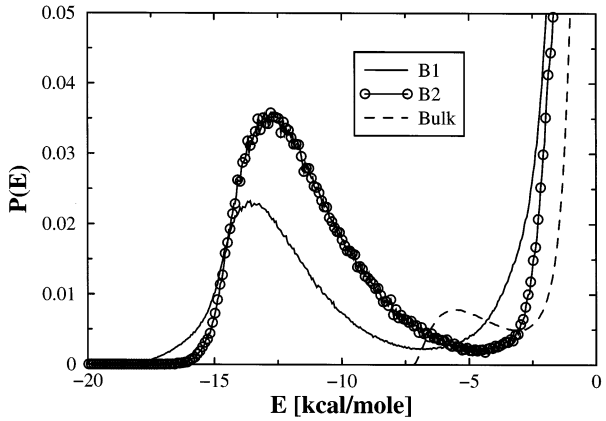


**Figure 5.** Potential-energy distributions for pairs of molecules; the term "Bulk" denotes pairs of water molecules in bulk. Here, "B1" and "B2" denote interfacial waters whose oxygen atoms are within 3.5 Å of one or two headgroups, respectively. Curves for B1 and B2 denote the distributions of potential energy of pairs of the type B1−PHG and B2−PHG. Alternate points are dropped in curves with symbols for clarity.

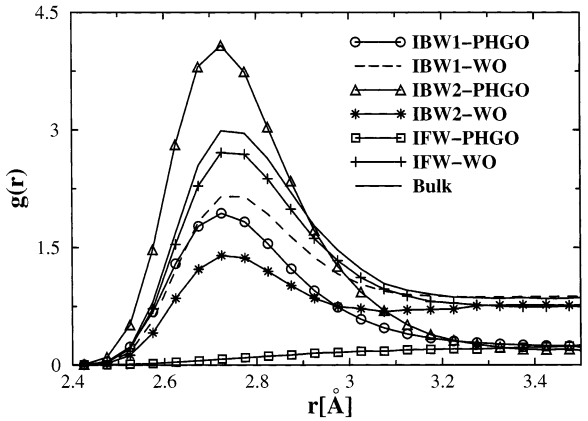


**Figure 6.** Various types of oxygen−oxygen radial distribution functions; the pair-correlation function ($g(r)$) values of interfacial waters with PHGO have been divided by a factor of 40.

of 3.5 Å can be rationalized as the position of the first minimum in the corresponding pair-correlation function, the specific choice for an angle cutoff of 30° appears to be somewhat arbitrary. However, this lacunae of a rationale can be redressed by the use of an energy cutoff in the hydrogen-bonding pair of molecules. To define such an energy cutoff, we first need to find out how the W−PHG interaction energies are distributed for interfacial water molecules, *in the absence of an angle or energy criterion*. We thus calculate the pair energy distribution of interfacial water molecules with PHGs, whose oxygen atoms are within 3.5 Å away from either one or two oxygen atoms of the PHG of any surfactant molecule. These data are presented in Figure 5 and compared to the distribution of the water−water potential energy in bulk water. The latter agrees well with earlier calculations.[41−43] The abscissa denotes the potential energy of the interaction of all sites on a water molecule with all three atoms (one carbon, and two oxygen) that constitute the headgroup of the surfactant. The tall peak near an energy value of zero comes from pairs that are separated by large distances, whereas the distinct peak at around −13.5 kcal/mol, with a minimum at −6.5 kcal/mol, denotes the hydrogen-bonding branch. This peak signifies pairs in close contact that are connected by a hydrogen bond. This energy minimum can be taken to define the energy cutoff of a hydrogen bond. Thus, we obtain a energy cutoff of −6.25 kcal/mol, weighting the respective minima of the two types of bound interfacial water molecules with their number concentration of ∼1:9. The results reported here will be unaffected, qualitatively—and, to a large extent, quantitatively—by the choice of either an energy or an angle condition in the definition of the hydrogen bond.

Thus, a W−PHG hydrogen bond is said to exist if the WO is within 4.35 Å of the headgroup carbon atom, and if the WO-to-PHGO distance is within a distance of 3.5 Å, and if the pair energy between a water molecule and a PHG is less than −6.25 kcal/mol.

We summarize the different types of water molecules as follows. (i) Interfacial water molecules are those that lie within 4.35 Å from the headgroup carbon atom of any surfactant molecule. (ii) Interfacial water molecules whose oxygen atom is within 3.5 Å from any headgroup, and whose pair energy with any headgroup is less than −6.25 kcal/mol, are denoted as IBW1 or IBW2; IBW1 molecules form one hydrogen bond with a surfactant, whereas IBW2 molecules form two hydrogen bonds with oxygen atoms of two different surfactant molecules. (iii) Interfacial water molecules that do not satisfy either (or both) of the distance and energy criteria described in (ii) are denoted as IFW.

Using these criteria, we observe the IFW:IBW1:IBW2 ratio to be 1.1:8.0:0.9. The fluidity of the solution phase, along with the fluctuations of the micellar surface, impart a dynamical equilibrium among these three species, and also with the water molecules in the bulk region of the micellar solution. Our aim is to characterize these species in terms of their structure and energetics. We now turn our attention to this aspect.

**3.3. Environment around Interfacial Water.** We have studied the pair-correlation functions, $g(r)$, of the oxygen atom of an interfacial water molecule with the oxygen atoms of other water molecules and also with the oxygen atoms of the PHG. These are displayed in Figure 6, along with the O−O $g(r)$ in pure water, for comparison. The first peak of the $g(r)$ of IFW, IBW1, or IBW2 with water oxygen atoms is shifted to a value of 2.725 Å, relative to the value of 2.775 Å in bulk water. This could arise from a possibly increased density of water at the hydrophilic surface. An accurate determination of the local density of water at the interface is difficult, in view of the roughness of the surface. The peak heights of the $g(r)$ of IBW1- and IBW2-type water molecules are reduced, relative to that of the IFW type, indicating the reduced coordination to other water molecules around the IBW1 and IBW2 species. The first peak in the WO−PHGO $g(r)$ for the IBW1 and IBW2 species also shown in the figure is located at a distance of 2.725 Å, and one can see the reduced intensity for the IBW1 species, relative to the IBW2 type, indicating that the loss of water molecules in the first coordination shell of IBW2 species is compensated by the hydrogen bonding to the PHGs. The water−water functions exhibit a first minimum at ∼3.2 Å, whereas the first minimum of the water−PHGO functions are located at 3.5 Å. The correlation function for IFW−PHGO is almost featureless. Its nonzero value within 3.5 Å arises from those water molecules which satisfy the two distance criteria but fail to satisfy the pair energy condition. It is likely that these water molecules, although present within 3.5 Å of the PHGO, are unfavorably oriented and, hence, are not hydrogen-bonded.

These conclusions are supported by the plots of the running coordination number obtained by integrating these pair-correlation functions, which are shown in Figure 7. To be consistent with the definition of hydrogen bond employed by other workers in studies of pure water,[34−36,39] we employ a common cutoff value of 3.5 Å for the discussion of the first coordination shell

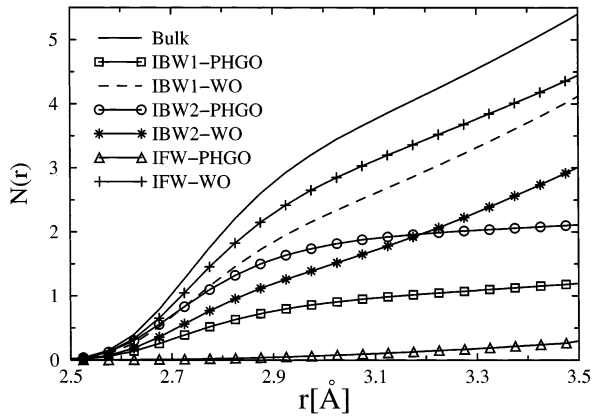


**Figure 7.** Running coordination numbers of oxygen atoms around oxygen atoms of interfacial water molecules, compared to data for bulk water.

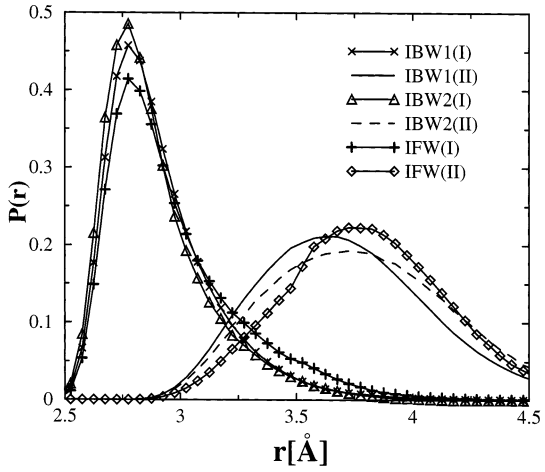


**Figure 8.** Distance distributions of the set of the four closest neighbors (denoted as "I" in parentheses) and that of the set of next four neighbors (denoted as "II" in parentheses) of different interfacial water molecules.

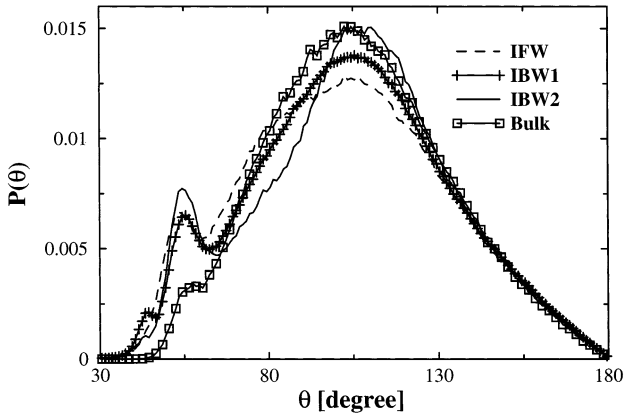


**Figure 9.** $O^IOO^I$ angle distribution ($P(\theta)$) for different interfacial water molecules and for bulk water. Alternate points are dropped in curves with symbols for clarity.

of an interfacial water molecule, despite small differences observed in the values of the first minima for water oxygen atoms and for the PHG oxygen atoms. Integrated up to 3.5 Å, the first coordination shell of an IFW species contains ∼4.4 water molecules and 0.3 PHG oxygen atoms, whereas that of the IBW1 species contains 4.1 water molecules and 1.2 PHGO atoms, and that of the IBW2 species contains 3.0 water molecules and 2.1 PHGO atoms. The residual 0.3 PHGO atoms in the coordination shell of IFW species comes from those water molecules that are within 3.5 Å but do not satisfy the energy condition. The number of PHGO atoms in the first coordination shell of the IBW1 and IBW2 species are not exact integers, for a similar reason. The total number of neighbors, irrespective of them being WO or PHGO, in the first coordination shell of IBW1 and IBW2 species is ∼5.2 but is considerably smaller for the IFW species, which are surrounded by only 4.7 oxygen atoms of either type. The IFW species are clearly undercoordinated, relative to the IBW1 or IBW2 species. In summary, it is seen that the surfactant headgroup substitutes cleanly for a water molecule in the first coordination shell of the bound interfacial water.

We can also obtain an idea about the near-neighbor shells by studying the distribution of neighbor distances, rather than the pair-correlation function. Such an analysis has been conducted in single-component systems earlier.[44] We have examined this quantity for interfacial water species, as shown in Figure 8. The collective set of the four closest neighbors is called type I, and the set of the next four neighbors is labeled type II. The identification of types I and II includes oxygen atoms from both water molecules, as well as from PHGs. The distributions of type I neighbors around an interfacial water molecule are almost identical for all the species, except for a subtle feature. The distribution narrows as one proceeds from IFW to IBW1 to IBW2. Thus, the near-neighbor distances for the IBW2 species are well defined, relative to the IBW1 and IFW species. The distribution for type II neighbors penetrates well into the first shell, indicating that the distinction between the first four neighbors and the second four is somewhat arbitrary, as the distances are continuously distributed. However, such a distinction is useful to understand the angle distributions within the first neighbor shell of an interfacial water.

The distribution of OOO angles in the type I shell, denoted as $O^IOO^I$, are shown in Figure 9. In bulk water, this distribution exhibits a peak near the tetrahedral angle of 109°, and a smaller peak at ∼55°. It is important to note the narrowing of the peak corresponding to tetrahedral neighbors for interfacial water molecules, relative to bulk water. This shows that the first neighbor shell of water is more sharply defined at the micelle−water interface than that for water in the bulk. The 55° peak is the angle between an occupant in the interstitial site around a water molecule and a tetrahedral neighbor. This shows that, at some instances, it is possible for the interstitial neighbor to be closer to the central water than a tetrahedral neighbor. This feature is accentuated for the interfacial water molecule, relative to the bulk water. The peak at 55° progressively increases in intensity for the IFW, IBW1, and IBW2 species, *indicating the increased presence of the interstitial neighbor in the first coordination shell of an interfacial water molecule*. The IBW1 and IBW2 species also exhibit a small peak at 43° that probably arises from their increased number of first neighbors. In combination with the distribution of near-neighbor distances data presented in Figure 8, we observe that *the environment around bound water species is more structured, relative to the free water*. This ties in with the observation of state energies of these species, which is discussed later.

Because of steric considerations, the IBW2 species cannot form two hydrogen bonds (through its two hydrogen atoms) with the two oxygen atoms of the same carboxylate unit. Rather, it forms hydrogen bonds with *two different surfactant molecules*. As expected, the occurrence of two headgroups at the proper distance and orientation, with respect to an interfacial water, is rare. This explains the low fraction of IBW2 species. In view of its unique bonding pattern, it is important to examine further the hydrogen bonds of the IBW2 species. We have studied the

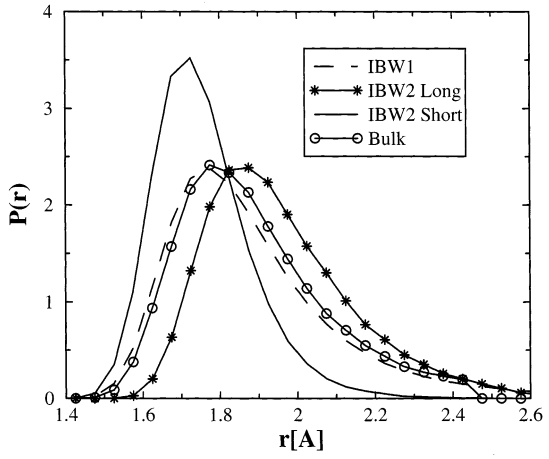


**Figure 10.** Distribution of hydrogen-bond lengths for hydrogen bonds involving IBW2, IBW1, and water molecules in bulk. IBW2 forms two hydrogen bonds with PHGO, and the distributions of the longer and shorter bonds are shown. IBW1 forms one hydrogen bond with PHGO.

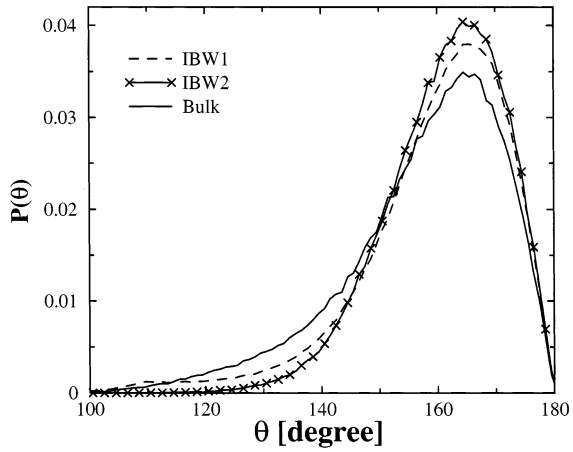


**Figure 11.** Distribution of hydrogen-bond angles (OHO) for hydrogen bonds involving IBW2, IBW1, and water molecules in bulk. Alternate points are dropped in curves with symbols for clarity.

distance distribution of the hydrogen bond length, i.e., the PHGO−WH bond length. We have calculated this quantity separately for the PHGO molecule that is closer to the oxygen atom of the IBW2 species and for the PHGO molecule that is farther from the IBW2 species. These distributions, which are shown in Figure 10, by virtue of their good separation, indicate that the two PHGO−IBW2 hydrogen bonds might be inequivalent. The average W−PHG hydrogen-bond lengths of the IBW2 species obtained from these distributions are 1.96 and 1.76 Å.

Having examined the hydrogen-bond lengths in the IBW2 species, we turn our attention to the angle of the hydrogen bond. We study the PHGO−WH−IWO angle distributions in Figure 11. A majority of the hydrogen bonds are almost linear, as observed from the peak at 165°. However, what is surprising is the rather long tail in this distribution for the hydrogen bond involving the PHG with the IBW1 species, relative to that in pure water. The tail is consistent with the increased presence of interstitial neighbors in the first coordination shell of an interfacial water, relative to that in pure water. Of more significance is the subtle difference in the angle distributions of IBW1 and IBW2 species, with the latter showing an unmistakable preference for linear hydrogen bonds over the former. The IBW2 molecule, in view of either its capability or necessity to form two hydrogen bonds with two different

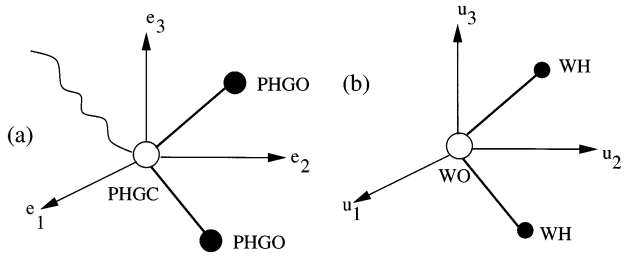


**Figure 12.** Schematic description illustrating the three vectors that define the orientation of the (a) PHG and (b) water molecule. Vectors $\vec{e}_1$ and $\vec{u}_1$ are normal to the plane of the PHG or the water molecule, whereas vectors $\vec{e}_2$, $\vec{u}_2$, $\vec{e}_3$, and $\vec{u}_3$ are in the plane of the PHG or the water molecule.

surfactant molecules, is constrained to form linear bonds with the PHGs. This results in a loss of its configurational entropy, an estimate of which we provide in the next subsection.

Significant structural differences between the IBW1 and IBW2 species exist in the way that their first shell neighbors are oriented relative to them. The orientation of any water molecule can be described by three vectors: (i) the dipole vector that bisects the two OH bonds; (ii) the vector that joins the two H atoms, which we call the HH vector; and (iii) the vector that passes through the O atom and is normal to the plane of the molecule. The PHG is similar to a water molecule in its geometry, with the PHGO being similar to WH, and the carbon atom of the PHG being similar to WO. We can again define three vectors that describe its orientation, in a manner similar to that for water. These vectors are schematically depicted in Figure 12. We are now interested in the relative orientations of the PHG in the first coordination shell, with respect to the orientation of the central, interfacial water molecule. We have calculated the distribution of the angle made between the dipole vector of a central interfacial water molecule and the dipole vector of the PHG to which it is bonded. Similar distributions of angles have been obtained for the vectors defined as (ii) in the previous discussion, and for the normals also. These distributions are compared to those obtained in bulk water in Figure 13. The distributions for bulk water involve angles between vectors defining the orientation of neighboring water molecules. In the cases of the angle between dipoles and that between the HH and OO vectors, the distributions of bound water species are quite different from that of bulk water. Although the PHG forms hydrogen bonds with water molecules whose characteristics are quite close to those formed between water molecules themselves, several differences between the two must be noted. In our model, the PHG is a charged entity, unlike a water molecule. Another crucial difference between the two is that the water−water hydrogen bond is one segment of a large, flexible, collective network that connects all the water molecules, whereas the W−PHG bond is more constrained. This fact, coupled with its larger strength (see later discussion) over the water−water hydrogen bond, induces different structural correlations, studied in the form of orientational correlations between an interfacial water molecule and its PHG neighbors. Let us now examine the data presented in Figure 13. The dipole−dipole angle distribution (Figure 13a) peaks at 122° for the IBW1 species and at the tetrahedral angle for the IBW2 water. The angle between the HH vectors of adjacent waters in bulk water peaks at 90°; however, the IBW1 distribution for the angle between WH−WH and PHGO−PHGO vectors exhibits a large plateau that is centered at ∼90° (Figure 13b). However, the same distribution acquires a special structure in the case of IBW2 water and exhibits two peaks, at 32° and 148°,

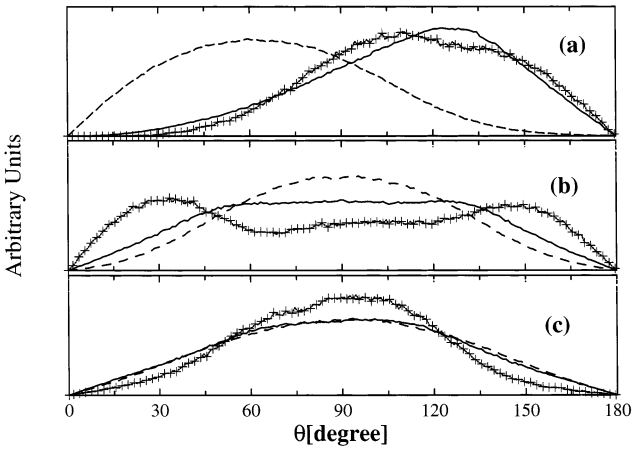


**Figure 13.** (a) Distribution of the angle between the vectors $\vec{e}_2$ and $\vec{u}_2$ for (−) IBW1 and (+) IBW2 for hydrogen-bonded neighbors; dashed line shows the distribution of angles between vectors $\vec{u}_2$ and $\vec{u}_2$ for hydrogen-bonded neighbors in bulk water. (b) Distribution of the angle between the vectors $\vec{e}_3$ and $\vec{u}_3$ for (−) IBW1 and (+) IBW2 for hydrogen-bonded neighbors; dashed line shows the distribution of angles between vectors $\vec{u}_3$ and $\vec{u}_3$ for hydrogen-bonded neighbors in bulk water. (c) Distribution of the angle between the vectors $\vec{e}_1$ and $\vec{u}_1$ for (−) IBW1 and (+) IBW2 for hydrogen-bonded neighbors; dashed line shows the distribution of angles between vectors $\vec{u}_1$ and $\vec{u}_1$ for hydrogen-bonded neighbors in bulk water. Alternate points are dropped in curves with symbols for clarity.

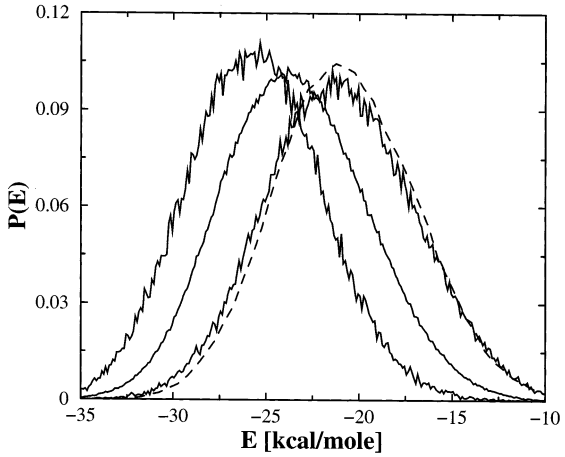


**Figure 14.** Distribution of monomer energies of interfacial water molecules (solid lines; from right to left, the IFW, IBW1, and IBW2 species) compared to that of bulk water (dashed line).

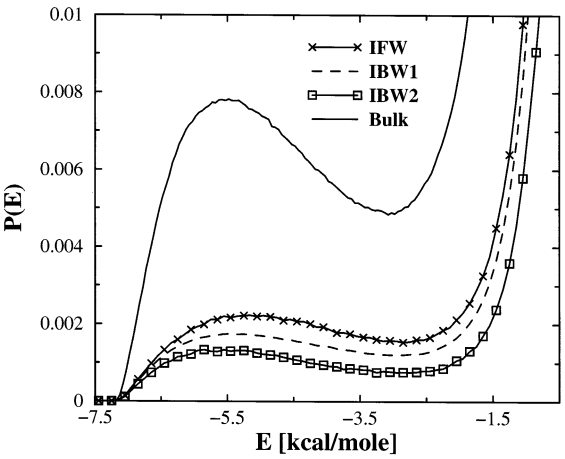


**Figure 15.** Potential-energy distributions for pairs of molecules; the term "Bulk" denotes pairs of water molecules in pure water. Curves for interfacial waters denote the distributions of potential energy of pairs of the type IBW1−water, IBW2−water, and IFW−water. Alternate points are dropped in curves with symbols, for clarity.

that are almost equal in height, indicative of the goodness of sampling of configurations in our simulations. The angle between the normal vectors exhibit a peak at ∼95° for all three cases (Figure 13c). The common factor that is associated with these three distributions is that the distribution for IBW2 is considerably narrower than those for the other two cases. The IBW2 species thus seems to be "structured" or "disciplined" in nature. The hydrogen bonds that it makes are more linear, and the IBW species forces its neighbors to approach it only in certain directions within a narrow window. It certainly does not seem to have the luxury of flexibility (or entropy) that a water molecule in bulk possesses.

**3.4. Energetics of Interfacial Water Species.** Data on the energetics of the interfacial water types provide more information regarding their state. The monomer or single-molecule energy distributions for the interfacial water molecules are shown in Figure 14 and are compared to that for pure water. The abscissa is the total interaction energy of a water molecule with the rest of the atoms in the micellar solution. The distribution for IFW species closely mirrors that in pure water, except for a nonnegligible shift of 0.5 kcal/mol toward lower energies. The IBW1 and IBW2 species are progressively more stable than the IFW species, with the state energy difference between IBW1 and IFW being 2.4 kcal/mol, and that between IBW2 and IBW1 being 1.7 kcal/mol. The increased stability of the IBW1 and IBW2 species could arise from their hydrogen bond with the PHGO. We first examine the strength of the hydrogen bond formed by the interfacial water molecules with other water molecules in the system. These dimer or pair energy distributions of interfacial water molecules are compared to that for bulk water in Figure 15. Note that the pairs examined in the figure are water−water in nature. The tall peak at zero energy arises from interacting pairs that are distant in the bulk. The distinct peak at approximately −5.5 kcal/mol is indicative of hydrogen bonding between water molecules. The decreased relative intensity of this peak for IFW, IBW1, and IBW2 waters comes from the reduced number of waters surrounding an interfacial water molecule. Clearly, the peak position remains unaltered and thus the strength of the water−water hydrogen bond for interfacial water molecules is the same as that in pure water, although the distributions for interfacial molecules are much broader. This could arise from the heterogeneous environments that the interfacial water molecules experience, relative to water molecules in bulk.

The previous discussion shows that the *increased stability* of the interfacial water molecules must come from their hydrogen bonding with the PHGs. The distribution of the energy between these pairs is shown in Figure 16, where the water−water pair energy distribution in bulk water is shown for comparison, to highlight the different energy scales. The abscissa is the total potential energy of interaction of a given water molecule type with all the atoms of a PHG. *A striking feature is that all the hydrogen bonds that the IBW1 and IBW2 make with PHG are stronger than the water−water hydrogen bond, by ∼7−8 kcal/mol*. This is the cause of the increased stability of these species, which is found in the monomer energy distribution. An additional significant observation is that, on the average, the hydrogen bonds of the IBW2 species with the PHGO are weaker than that formed by the IBW1 species with the PHGO, by ∼1 kcal/mol. This remarkable result is consistent with our observations on the constrained geometry of the IBW2

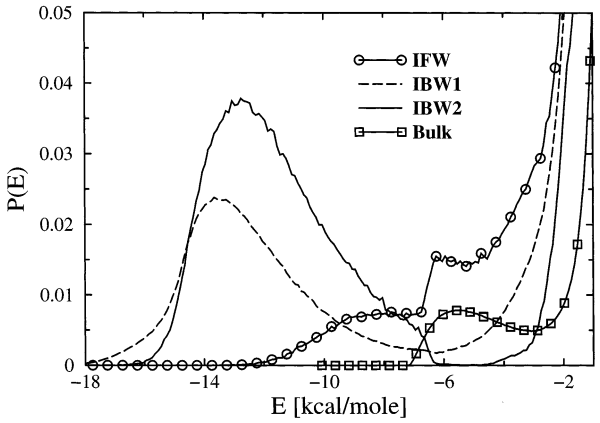


**Figure 16.** Potential-energy distributions for pairs of molecules of the type IBW1−PHG, IBW2−PHG, and IFW−PHG. Three out of four points are dropped in the curve with symbols, for clarity. The apparent discontinuity in the curve for IFW−PHG at −6.25 kcal/mol is an artifact resulting from the use of this value as the energy cutoff in defining IFW. The pair energy distribution in bulk water is shown for comparison.

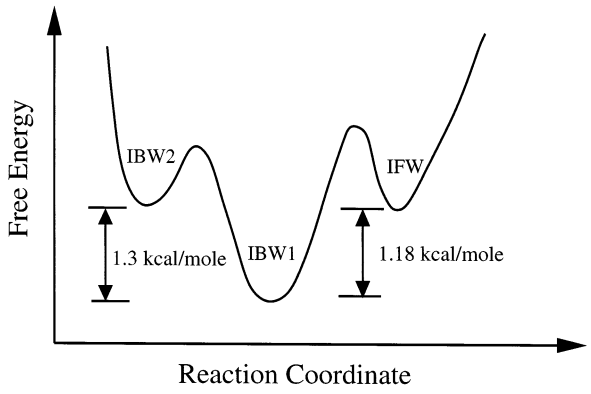


**Figure 17.** Schematic description of the free-energy profile of the interfacial water species. The species are in dynamical equilibrium with themselves and with water present in the bulk region of the micellar solution. The reaction coordinate is arbitrary and does not imply any distance. Barrier heights also are arbitrary.

species discussed earlier. The IBW2 species derives its increased stability, relative to the IBW1 species, from the fact that it forms two hydrogen bonds with PHGO, *despite each of them being weaker individually than the one hydrogen bond that an IBW1 species forms with PHGO*. Another factor that is likely to have contributed to the pair-energy difference between IBW1 and IBW2 is the existence of subtle structural differences between the two species. For instance, one of the PHGO that is not bonded to an IBW2 species is present predominantly at a distance of 4.7 Å from the water oxygen atom, whereas the IBW1 species is devoid of any such environment. As discussed in Figure 13, the orientation of the PHG, with respect to the IBW2 water, is different from that for the IBW1 water. Such structural differences at non-nearest-neighbor distances contribute to the weakening of the pair interaction energy of an IBW2 water with a PHG to which it is hydrogen-bonded. The pair energy distribution of the IFW species shows a broad hump at approximately −8.5 kcal/mol which arises from those interfacial waters that satisfy the energy condition but fail the distance criterion. The feature above −5.5 kcal/mol comes from those IFW species that fail the energy condition and may or may not have passed the distance condition. What is significant is that the IFW species, by virtue of its electrostatic interactions with the proximal surfactant molecules, gains in stabilization energy, relative to water in the bulk.

## 4. Conclusions

We have investigated the microscopic nature of water in a micelle−water interface, the dynamics of which we have studied earlier.[17−21] We have presented evidence for the stability of the micelle, and for the penetration of water molecules that soak a couple of CF2 groups below the headgroup of the surfactant. This feature also has been reported in a large number of other simulations.[22,23] Using a definition of the hydrogen bond between an interfacial water molecule and the polar headgroup (PHG) of the surfactant, we find the existence of three types of waters at the interface, based on the number of hydrogen bonds they make with the headgroup oxygen atoms. The three species (those formed without any hydrogen bonds (IFW), those forming one hydrogen bond to a PHG (IBW1), and those forming two hydrogen bonds to two different PHGs (IBW2)), in dynamical equilibrium with each other and with bulk water, are present in the respective ratio of 1.1:8.0:0.9, with a predominance of water molecules that are singly hydrogen-bonded to PHGs.

The average concentration of these species can be used to calculate the equilibrium constants of the reversible reactions between IBW2 and IBW1 on one hand, and between IBW1 and IFW on the other. These equilibrium constants can then provide the free-energy differences between the three species. We provide, in Figure 17, a schematic description of these data, obtained on the lines previously described . Despite possessing two strong W−PHG bonds, the concentration of the IBW2 species is rather low. This indicates that entropy has a significant role in determining the free-energy differences and, thus, the concentration ratios. From the free-energy and monomer energy data, we estimate the entropy loss of the IBW2 species over the IBW1 species to be 10 cal/mol/K.[45] This loss of entropy for the IBW2 type of molecules is evidently related to the previously described structural observations. We have seen that the IBW2 species favors more-linear hydrogen bonds with the PHG and has a significantly different relative orientation of PHG groups in its first coordination shell. In addition, neighboring waters prefer to surround an IBW2 water in a tetrahedral geometry better than how they do around an IBW1 water. These constraints decrease the flexibility of this water species, thus reducing its entropy. The rarity of two PHGs coming together at the right distance and orientation for an interfacial water molecule to form bonds also decreases the entropy contribution, thus increasing the free energy of the IBW2 state, with respect to the IBW1 species. Dynamical consequences of these aspects and the rates at which the reversible reactions between the three interfacial species occur, will be explored in the future.

In the present work, we have additionally characterized the environment around these species. We find that the first neighbor shell of the interfacial water molecule is structured in a well-defined manner, relative to a water molecule in bulk. This is observed in the narrowing of the OOO angle distribution, corresponding to tetrahedral neighbors. In addition, we find evidence for an increase in the occupation of the interstitial site for interfacial water, as compared to bulk water. Consequently, the OHO angle distribution shows a significant tail up to 100° in the case of IBW1 water that is present only weakly in bulk water.

We have shown that the IBW2 species, which forms two hydrogen bonds with two different surfactant molecules, is geometrically constrained and that the two hydrogen bonds are not equivalent. This is also confirmed by a study on the energetics of the water molecules themselves and the energy

distributions of the hydrogen-bonded pairs. A significant discovery of the present work is the demonstration that the average energy of the hydrogen bond formed by an IBW2 species with the PHG is weaker than that formed by an IBW1 species, by ~1 kcal/mol. This finding should help in understanding the dynamics of interfacial molecules themselves,[46] and also the rates at which they interconvert. In general, an interfacial water is energetically more stable than bulk water, which will influence its ability to translate and, possibly, reorient. Thus, the current set of results that we have presented here adds substantive microscopic perspective on the origin of the slow dynamics in aqueous interfaces that has been observed earlier in experiments and in our simulations.

A note on the impact of the choice of hydrogen-bonding criteria on our results is in order. As discussed earlier, the choice of a distance condition between the oxygen atoms can be guided by their pair-correlation function. However, the choice of an angular condition that determines the cutoff in the angle of OOH or OHO is less unambiguous. Various workers have used a 30° cutoff in the definition of the water−water hydrogen bond, despite the knowledge that the choice is somewhat arbitrary.[34−36] We find that a more robust definition of the hydrogen bond could be based on its energy. The fact that a large fraction of the interfacial water molecules are found to form linear hydrogen bonds shows that the energy criterion used here is reasonable. Thus, the results discussed here will qualitatively—and, to a large extent, quantitatively should—remain invariant to the choice of an energy or angular cutoff.

The micelle−water interface shares a large commonality with interfaces formed by biologically relevant macromolecules. Hence, we expect many of our observations on the identity, structure, and energetics of the interfacial species to be relevant, even to those complex systems. There are, of course, some crucial differences, such as, although the interface in the micellar solution is chemically homogeneous, that in an aqueous protein solution has a large chemical heterogeneity. The latter will influence local pockets of water, in a manner which could be different. Another difference is that the protein conformation is more rugged and complex than the micellar surface. This may also influence the rate at which different species exchange with bulk water. It is difficult to predict the ratio of bound-to-free water species in the hydration layer of proteins. Given the presence of less polar and hydrophobic residues in the protein, we expect a larger concentration of free water species in such systems than what has been reported here for a micelle with a polar, hydrophilic surface. Work in this direction is under progress.

**Acknowledgment.** We (S.B. and B.B.) thank the Council of Scientific and Industrial Research, and Department of Science and Technology, India, for financial support.

## References and Notes

(1) Lee, S. H.; Rossky, P. J. *J. Chem. Phys.* **1994**, *100*, 3334.
(2) Vajda, S.; Jimenez, R.; Rosenthal, S. J.; Fidler, V.; Fleming, G. R.; Castner, E. W., Jr. *J. Chem. Soc., Faraday Trans.* **1995**, *91*, 867.
(3) Scodinu, A.; Fourkas, J. T. *J. Phys. Chem. B* **2002**, *106*, 10292.
(4) Bandyopadhyay, S.; Tarek, M.; Klein, M. L. *Curr. Opin. Colloid Interface Sci.* **1998**, *3*, 242.
(5) Cheng, Y.-K.; Rossky, P. J. *Nature* **1998**, *392*, 696.
(6) Tarek, M.; Tobias, D. J. *Phys. Rev. Lett.* **2002**, *88*, 138101.
(7) Nandi, N.; Bhattacharyya, K.; Bagchi, B. *Chem. Rev.* **2000**, *100*, 2013.
(8) (a) Ringe, D. *Curr. Opin. Struct. Biol.* **1995**, *5*, 825. (b) Sansom, M. S. P.; Srivastava, I. H.; Ranatunga, K. M.; Smith, G. R. *Trends Biochem. Sci.* **2000**, *25*, 368. (c) Teeter, M. M.; Yamano, A.; Stec, B.; Mohanty, U. *Proc. Natl. Acad. Sci.* **2001**, *98*, 11242. (d) Mattos, C. *Trends Biochem. Sci.* **2002**, *27*, 203. (e) Pratt, L. R.; Pohorille, A. *Chem. Rev.* **2002**, *102*, 2671. (f) Marchi, M.; Sterpone, F.; Ceccarelli, M. *J. Am. Chem. Soc.* **2002**, *124*, 6787. (g) Ruffle, V.; Michalarias, I.; Li, J.; Ford, R. C. *J. Am. Chem. Soc.* **2002**, *124*, 565.
(9) Sarkar, N.; Dutta, A.; Das, S.; Bhattacharyya, K. *J. Phys. Chem.* **1996**, *100*, 15483.
(10) Riter, R. E.; Willard, D. M.; Levinger, N. E. *J. Phys. Chem. B* **1998**, *102*, 2705.
(11) Mandal, D.; Sen, S.; Sukul, D.; Bhattacharyya, K. *J. Phys. Chem. B* **2002**, *106*, 10741.
(12) (a) Faeder, J.; Ladanyi, B. M. *J. Phys. Chem. B* **2000**, *104*, 1033. (b) Faeder, J.; Ladanyi, B. M. *J. Phys. Chem. B* **2001**, *105*, 11148.
(13) Fukuzaki, M.; Miura, N.; Sinyashiki, N.; Kunita, D.; Shiyoya, S.; Haida, M.; Mashimo, S. *J. Phys. Chem.* **1995**, *99*, 431.
(14) Jordanides, X. J.; Lang, M. J.; Song, X.; Fleming, G. R. *J. Phys. Chem. B* **1999**, *103*, 7995.
(15) Otting, G. In *Biological Magnetic Resonance*; Ramakrishna, N., Berliner, L. J., Eds.; Kluwer Academic/Plenum: New York, 1999; Vol. 17, p 485.
(16) Nandi, N.; Bagchi, B. *J. Phys. Chem. B* **1997**, *101*, 10954.
(17) Balasubramanian, S.; Bagchi, B. *J. Phys. Chem. B* **2002**, *106*, 3668.
(18) Pal, S.; Balasubramanian, S.; Bagchi, B. *J. Chem. Phys.* **2002**, *117*, 2852.
(19) Balasubramanian, S.; Bagchi, B. *J. Phys. Chem. B* **2001**, *105*, 12529.
(20) Balasubramanian, S.; Pal, S.; Bagchi, B. *Curr. Sci.* **2002**, *82*, 845.
(21) Balasubramanian, S.; Pal, S.; Bagchi, B. *Phys. Rev. Lett.* **2002**, *89*, 115505.
(22) Watanabe, K.; Klein, M. L. *J. Phys. Chem.* **1991**, *95*, 41581.
(23) Shelley, J. C.; Sprik, M.; Klein, M. L. *Langmuir* **1993**, *9*, 916.
(24) Mackerell, A. D., Jr. *J. Phys. Chem.* **1995**, *99*, 1846.
(25) Boden, N.; Jolley, K. W.; Smith, M. H. *J. Chem. Phys.* **1993**, *97*, 7678.
(26) Iijima, H.; Kato, T.; Yoshida, H.; Imai, M. J. *J. Phys. Chem. B* **1998**, *102*, 990.
(27) Gelbart, W. M.; Ben-Shaul, A. *J. Phys. Chem.* **1996**, *100*, 13169.
(28) Berendsen, H. J. C.; Grigera, J. R.; Straatsma, T. P. *J. Chem. Phys.* **1987**, *91*, 6269.
(29) Sprik, M.; Röthlisberger, U.; Klein, M. L. *Mol. Phys.* **1999**, *97*, 355.
(30) Tuckerman, M. E.; Berne, B. J.; Martyna, G. J. *J. Chem. Phys.* **1992**, *97*, 1990.
(31) Tuckerman, M. E.; Yarne, D. A.; Samuelson, S. O.; Hughes, A. L.; Martyna, G. J. *J. Comput. Phys. Commun.* **2000**, *128*, 333.
(32) Stillinger, F. H. *Adv. Chem. Phys.* **1975**, *31*, 1.
(33) Rapaport, D. C. *Mol. Phys.* **1983**, *50*, 1151.
(34) Ferrario, M.; Haughney, M.; McDonald, I. R.; Klein, M. L. *J. Chem. Phys.* **1990**, *93*, 5156.
(35) (a) Luzar, A.; Chandler, D. *J. Chem. Phys.* **1993**, *98*, 8160. (b) Luzar, A.; Chandler, D. *Phys. Rev. Lett.* **1996**, *76*, 928. (c) Luzar, A.; Chandler, D. *Nature* **1996**, *379*, 53.
(36) Starr, F. W.; Nielsen, J. K.; Stanley, H. E. *Phys. Rev. E* **2000**, *62*, 579.
(37) Chandra, A. *Phys. Rev. Lett.* **2000**, *85*, 768.
(38) Xu, H.; Berne, B. J. *J. Phys. Chem. B* **2001**, *105*, 11929.
(39) Svishchev, I. M.; Kusalik, P. G. *J. Chem. Phys.* **1993**, *99*, 3049.
(40) Bruce, C. D.; Senapati, S.; Berkowitz, M. L.; Perera, L.; Forbes, M. D. E. *J. Phys. Chem. B* **2002**, *106*, 10902.
(41) Rahman, A.; Stillinger, F. H. *J. Chem. Phys.* **1971**, *55*, 3336.
(42) Jorgensen, W. L.; Chandrasekhar, J.; Madura, J. D.; Impey, R. W.; Klein, M. L. *J. Chem. Phys.* **1983**, *79*, 926.
(43) Balasubramanian, S.; Mundy, C. J.; Klein, M. L. *J. Chem. Phys.* **1996**, *105*, 11183.
(44) Saitta, A. M.; Datchi, F. *Phys. Rev. E* **2003**, *67*, 020201.
(45) Smith, J. C.; Merzel, F.; Verma, C. S.; Fischer, S. *J. Mol. Liq.* **2002**, *101*, 27.
(46) Pal, S.; Balasubramanian, S.; Bagchi, B. *Phys. Rev. E*, in press.